

F/G 11/6

THE SIZE AND DENSITY OF INTERGRANULAR

DAAG29-80-K-0045

ARO-17221.1-E

NL

1 of 1

END
DATE
FILMED
4-81
DTIC

AD A 097022

DTIC FILE COPY

UNCLASSIFIED
SECURITY CLASSIFICATION OF THIS PAGE (When Data Entered)

REPORT DOCUMENTATION PAGE		READ INSTRUCTIONS BEFORE COMPLETING FORM
1. REPORT NUMBER 17221.1-E	2. GOVT ACCESSION NO. AD-4097022	3. RECIPIENT'S CATALOG NUMBER
4. TITLE (and Subtitle) The Size and Density of Intergranular Carbide Plates in 1020 HRS and Their Role During Brittle Fracture Initiation: A Preliminary Report	5. TYPE OF REPORT & PERIOD COVERED Technical	
7. AUTHOR(s) J. C. Lambropoulos R. J. Asaro R. H. Hawley	6. PERFORMING ORG. REPORT NUMBER	
9. PERFORMING ORGANIZATION NAME AND ADDRESS Brown University Providence, RI 02912	8. CONTRACT OR GRANT NUMBER(s) DAAG29-80-K-0045	
11. CONTROLLING OFFICE NAME AND ADDRESS U. S. Army Research Office Post Office Box 12211 Research Triangle Park, NC 27709	10. PROGRAM ELEMENT, PROJECT, TASK AREA & WORK UNIT NUMBERS 10251	
14. MONITORING AGENCY NAME & ADDRESS (if different from Controlling Office)	12. REPORT DATE 11 Jan 81	
	13. NUMBER OF PAGES 22	
	15. SECURITY CLASS. (of this report) Unclassified	
15a. DECLASSIFICATION/DOWNGRADING SCHEDULE		
16. DISTRIBUTION STATEMENT (of this Report) Approved for public release; distribution unlimited.		
17. DISTRIBUTION STATEMENT (of the abstract entered in Block 20, if different from Report) NA		
18. SUPPLEMENTARY NOTES The view, opinions, and/or findings contained in this report are those of the author(s) and should not be construed as an official Department of the Army position, policy, or decision, unless so designated by other documentation.		
19. KEY WORDS (Continue on reverse side if necessary and identify by block number) carbides grain boundaries fracture properties strain rate microstructure mechanical properties steel fracture toughness		
20. ABSTRACT (Continue on reverse side if necessary and identify by block number) The purpose of this investigation is to determine the effect of microstructure on the dynamic and quasi-static fracture initiation in a plain carbon steel. For this purpose experiments were conducted on an AISI 1020 steel with either of two microstructures, the first a normalized microstructure, and the second an isothermally transformed (at 550°C) ferritic-pearlitic microstructure. An important distinction between these microstructures is the resulting density and size of grain boundary carbides that are found to initiate cleavage cracks. The high rate fracture toughness		

DD FORM 1 JAN 73 1473 EDITION OF 1 NOV 65 IS OBSOLETE

UNCLASSIFIED
SECURITY CLASSIFICATION OF THIS PAGE (When Data Entered)

81 3 23 138

4/16/81

testing method employed was developed only recently. Tests were conducted over the temperature range -130C to 65C. The fracture toughness tests were complemented by high rate and quasi-static plasticity tests to provide necessary data on the mechanical behavior of both microstructures over the same temperature range and over approximately the same range of strain rates. Results show that the isothermally transformed microstructure is both stronger and tougher than the normalized microstructure at temperatures below about 18°C where cleavage occurs. This appears to be due to the reduction in density of grain boundary carbides. At temperatures above 18°C the fracture mode is fibrous in both microstructures and the toughnesses of the two microstructures are comparable. The quasi-static strength of the isothermally transformed microstructure is higher but the strength at higher strain rates is a little lower at temperatures above 18°C.

Classification

Exemption Codes

Review and/or Special

12

DIVISION OF ENGINEERING
BROWN UNIVERSITY
PROVIDENCE, RI

THE SIZE AND DENSITY OF INTERGRANULAR CARBIDE PLATES IN 1020 HRS
AND THEIR ROLE DURING BRITTLE FRACTURE INITIATION: A PRELIMINARY REPORT

J. C. LAMBROPOULOS, R. J. ASARO, R. H. HAWLEY, AND J. DUFFY

MATERIALS RESEARCH LABORATORY
BROWN UNIVERSITY

ARMY RESEARCH OFFICE
RESEARCH TRIANGLE PARK, NC 27709

ARO DAAG29-80-K-0045/1

JANUARY, 1981

Abstract

The purpose of this investigation is to determine the effect of microstructure on the dynamic and quasi-static fracture initiation in a plain carbon steel. For this purpose experiments were conducted on an AISI 1020 steel with either of two microstructures, the first a normalized microstructure, and the second an isothermally transformed (at 550°C) ferritic-pearlitic microstructure. An important distinction between these microstructures is the resulting density and size of grain boundary carbides that are found to initiate cleavage cracks.

The high rate fracture toughness testing method employed was developed only recently and provides a stress intensity rate, \dot{K}_I , of approximately $2 \times 10^6 \text{ MPa } \sqrt{\text{m}} \text{ s}^{-1}$. Tests were conducted over the temperature range -130°C to 65°C. The fracture toughness tests were complemented by high rate and quasi-static plasticity tests to provide necessary data on the mechanical behavior of both microstructures over the same temperature range and over approximately the same range of strain rates. Results show that the isothermally transformed microstructure is both stronger and tougher than the normalized microstructure at temperatures below about 18°C where cleavage occurs. This appears to be due to the reduction in density of grain boundary carbides. At temperatures above 18°C the fracture mode is fibrous in both microstructures and the toughnesses of the two microstructures are comparable. The quasi-static strength of the isothermally transformed microstructure is higher but the strength at higher strain rates is a little lower at temperatures above 18°C.

I. Introduction

A number of experimental investigations have been carried out recently concerned with the role of microstructure in the fracture of low carbon steels and in particular on steels that fail by cleavage. Several of these studies have led to a phenomenological description of cleavage which involves the initiation of cleavage cracks at grain boundary carbides when critically high stresses (or strains) are attained, and the propagation of these cracks through the ferrite matrix [1-4]. If one considers the tip of an existing crack or notch with its characteristic non-uniform stress-strain field, then an associated fracture criterion which follows is found by stating that this critically high stress (or strain) must be achieved over microscale distances which include the crack initiating sites; the stress intensity required to accomplish this is K_{IC} . For example, Ritchie et al. [5] were successful in explaining the temperature dependence of K_{IC} in a mild steel by arguing that the critical fracture stress was essentially independent of temperature and by accounting for the temperature dependence of the material's flow stress--a decrease in flow stress accompanying an increase in temperature requires a higher applied stress intensity to achieve the critical stress over the critical distance, and thus leads to an increase in toughness. Costin and Duffy [3] were also successful in explaining the temperature dependence of K_{IC} under conditions of high rates as well as quasistatic loading for a plain carbon steel which fractured by cleavage. In both of these studies the critical distance was found to be comparable to the average grain boundary carbide spacing consistent with the phenomenological model described above.

The present study was undertaken in order to further explore the role of microstructure in a plain carbon 1020 steel in both quasi-static and high rate fracture and, in particular, to explore the role of carbide morphology on

fracture toughness. Two carbide morphologies were studied, one produced by the isothermal transformation of austenite and the other by a normalization. The size and density of isolated grain boundary carbides were approximately a factor of two less in the isothermally transformed microstructure than in the normalized microstructure, whereas the volume fraction of pearlite and the average ferrite grain size were nearly the same. The results are consistent with the model in that at temperatures less than approximately 18°C the fractures are by cleavage and the fracture toughness of the isothermally transformed steel is higher than that of the normalized steel. At temperatures above 18°C, the fractures involve void growth and coalescence and the toughnesses of the two microstructures are comparable.

II. Experimental

Fracture Toughness Tests

The apparatus used in the present experiment is an adaptation of the Kolsky bar due to Costin et al. [6]. Since the apparatus is described in detail by those authors the description given below is brief; it also makes use of their figures as well as those of a later paper by Wilson et al. [4]. The experimental arrangement is shown schematically in Fig. 1. The specimen consists of a round bar with a pre-cracked fatigue notch located 76 cm from one end. Specimen dimensions are shown in Fig. 2.

Loading is accomplished by means of an explosive charge detonated against a mass attached at the end of the bar as shown in Fig. 1. A tensile pulse is thus initiated which propagates to the notch to produce the fracture. This tensile pulse has a rise-time of 35-40 microseconds at the fracture site. Typically fracture of the specimen occurs during the rising portion of the pulse, about 20-25 microseconds after its arrival. The average stress at

the fracture site is measured as a function of time by means of strain gages mounted on the further side of the notch, as in the Kolsky bar. The crack opening displacement (COD) is determined as a function of time through the use of Moire fringes as described in [6]. We thus have all the necessary information to calculate the value for K_{Ic} , except the instant of fracture initiation.

For brittle fracture, the instant of fracture initiation coincides with the peak load, but it departs somewhat from this for more ductile fractures [3,4,6]. In either case, the time of fracture initiation is determined by examining the reflected pulse, as monitored by strain gages mounted on the near side of the notch. Since the magnitude of this pulse depends on the ratio of the ligament's cross-sectional area to that of the specimen, a sharp change in the reflected pulse occurs for a brittle fracture. However, when the fracture becomes more ductile the instant of fracture initiation becomes more difficult to establish with precision. The resulting error in time can produce a sizable error in the calculated critical value of the stress intensity factor which now becomes the J-integral, J_{Ic} [3,4]. This possible error in J_{Ic} should be kept in mind when examining results of ductile fracture tests.

Quasi-static fracture tests were conducted with the same specimen configuration and the same instrumentation as used in the dynamic tests, by loading the specimen in tension in a universal testing machine. Both dynamic and quasi-static tests were conducted over the temperature range -130°C to 65°C ; cooling was effected by the use of an environmental chamber and liquid nitrogen.

Plasticity Tests

The mechanical properties of low carbon steels are quite sensitive to rate of deformation and to temperature. Hence, in the analysis of the results of

dynamic fracture tests it is necessary to take into account, at least approximately, the increase in flow stress which results from the high strain rates encountered in these tests, as well as its dependence on test temperature.

Accordingly, plasticity experiments were performed to determine the quasi-static and dynamic stress-strain curves for the 1020 HRS, both normalized and following the isothermal transformation. These results are shown in Fig. 5(a)-5(c).

They were obtained by testing specimens of the two metals in shear by means of a torsional Kolsky bar. Only a brief description of this apparatus is presented below since all details can be found in Senseny et al. [7].

A schematic diagram showing the torsional Kolsky bar is shown in Fig. 3 and a typical specimen in Fig. 4. As may be seen, the specimen consists of a thin-walled tube with a gage length of 2.5 mm, an inside diameter of 9.5 mm and a wall-thickness of 0.38 mm. It is machined out of a single piece of metal stock with two hexagonal flanges used for gripping. The specimen is mounted at C, near the center of the Kolsky bar, into closely fitting hexagonal sockets. In addition, each flange is prevented from rotating by a group of six set screws each of which bears down on a hexagonal surface. (Separate tests show that there is virtually no change in torsional impedance with this method of gripping the flange.) The apparatus can provide either a quasi-static or a dynamic strain rate. The dynamic rate is obtained by first storing a torque T between pulley A and clamp B, and then suddenly releasing the clamp to allow a torsional pulse of amplitude $T/2$ to propagate toward the specimen. The length of this pulse is equal to twice the distance from A to B. Strain gages at G provide a measure of the torque transmitted through the specimen, while those at F give the reflected pulse. As in the standard Kolsky bar [8], the first of these signals can be calibrated in terms of shear stress in the specimen as a function of time and the second

as shear strain rate. An integration gives shear strain, and by eliminating time one obtains a shear stress-shear strain curve with the strain rate determined at each point. As mentioned above, quasi-static loading can also be performed with this apparatus. This is done simply by turning the pulley D while holding the bar clamped at B. For the static test, stress is calculated from the applied torque as measured at G, while the strain is deduced from the relative angular displacements of the two ends of the specimen as measured by means of direct current differential transformers. Thus, the same apparatus and the same geometry of specimen are used for quasi-static and dynamic testing. The respective strain rates are $5 \cdot 10^{-4} \text{ s}^{-1}$ and 1000 s^{-1} .

Material

The 1020 steel used in the present experiments was received in the form of 1 inch diameter rods with the composition listed in Table I; the microstructure was normalized and is referred to as microstructure N in what follows. A second microstructure (referred to as I) was produced by austenitizing the as-received material for 1 hour at 950°C followed by a quench to 550°C in a lead bath and isothermal transformation for 30 minutes. Some relevant microstructural details are listed in Table II. As shown in the Table, there was a noticeable difference in both the size and spacing of isolated carbides on the ferrite grain boundaries; this has important implications for the initiation of cleavage.

Method of Data Analysis

The data analysis follows that of Costin et al. [6]. For a nominally brittle fracture, the stress intensity factor has been evaluated by Tada [9] as

$$K_I = (P/\pi R^2) \sqrt{\pi R} F(2R/d) \quad (1)$$

where P is the applied load, R is the radius of the remaining circular

ligament after fatigue, D is the outer diameter of the bar, and $F(2R/D)$ is a size function which in the present instance equals approximately 0.48.

To insure a valid K_{Ic} test, we use the criterion

$$R \geq 2.5 (K_{Ic}/\sigma_y)^2 \quad (2)$$

where σ_y is the flow stress of the material at a temperature and strain rate comparable to those occurring during fracture initiation. When the fracture is not brittle, an equivalent stress intensity factor K_{Jc} can be found from

$$K_{Jc} = \left[\frac{EJ_{Ic}}{1-\nu^2} \right]^{1/2} \quad (3)$$

where E is Young's modulus, ν is Poisson's ratio, and J_{Ic} is the critical value of the J -integral given by Rice et al. [10] as

$$J = \frac{1}{2\pi R^2} \left[3 \int_0^{\delta_c^*} P d\delta_c - P^* \delta_c^* \right] \quad (4)$$

where δ_c is the load-point displacement due to the presence of the crack, and the asterisk indicates that the quantity is evaluated at the instant of fracture initiation. The load-point displacement can be approximated by the crack opening displacement determined from the load displacement curve. Costin et al. [6] showed that the error introduced by this approximation is not significant.

III. Results

Plasticity

Representative stress-strain data at shear strain rates of $5 \times 10^{-4} \text{ s}^{-1}$ and 10^3 s^{-1} are shown in Figures 5(a)-5(c). As indicated by the data, at these two strain rates the yield stress and the strain hardening characteristics of the two microstructures, N and I , are comparable, although the isothermally transformed microstructure is usually somewhat stronger. This is not surpris-

ing considering the similarity in the volume fractions and average grain size of ferrite and the pearlitic regions. The only case in which a significant difference in strength and flow characteristics appeared was in the high rate tests carried out at 18°C, where the isothermally transformed microstructure was considerably (roughly 40 percent) higher in strength than the normalized microstructure.

Fracture Mode

Under high rate conditions, both the isothermally transformed and normalized microstructures show essentially a transgranular cleavage mode of fracture, at least within the temperature range -130°C to 18°C. SEM fractographs showing this cleavage in the isothermally transformed steel are presented in Fig. 6. These indicate that cleavage initiated at the grain boundary carbides in both microstructures. Above 18°C fracture initiation was more ductile and involved void initiation and growth; the fracture surfaces showed no evidence of cleavage.

Fracture Toughness

In Fig. 7 the values of K_{IC} are plotted for both microstructures over the entire temperature range. As stated above, below about 18°C the fracture mode was transgranular cleavage which initiated predominantly at grain boundary carbides. The fracture toughness of the isothermally transformed microstructure was uniformly higher over the temperature range -130°C to 18°C, i.e. within the cleavage regime, whereas above 18°C, where the fracture mode was more ductile, the toughness of the two microstructures was approximately equal. The present results suggest then, that the isothermally formed microstructure is more resistant to cleavage at the lower temperatures but that the microstructures display very similar behavior at higher temperatures, where the fractures are more ductile and involve void initiation and growth.

IV. Discussion

Our results for the fracture toughness in the temperature range where fracture is by cleavage are consistent with the model described in the Introduction. To see this, we consider McMeeking's calculation of the crack tip stress field shown in Fig. 8 [11]. The critical cleavage stress, σ_{yy}^* , determines a critical ratio σ_{yy}^*/σ_y which corresponds to a certain intercept I^* on the R/b axis. The fracture criterion can be phrased as

$$(R/b)^* = I^* . \quad (5)$$

Since this critical value of σ_{yy} must extend over a minimum physical extent, δ^* , we identify R in the above as $R = \delta^*$; the fracture criterion now becomes

$$\delta^*/b^* = I^* \quad \text{or} \quad (6a)$$

$$b^* = \delta^*/I^* . \quad (6b)$$

Now, for a material of comparable strength and strain hardening capacity, McMeeking's calculations suggest that $b \approx 0.5 J/\sigma_y$ where, for small scale yielding, $J = (1 - \nu^2)K^2/E$. Thus, identifying K^* with K_{Jc} , we obtain $0.5(1 - \nu^2) K_{Jc}^2/(E\sigma_y) \approx \delta^*/I^*$ or

$$K_{Jc} = \sqrt{\frac{2\delta^*E\sigma_y}{(1-\nu^2)I^*}} \quad (7)$$

It should be noted that I^* typically increases strongly with σ_y (or actually with decreasing σ_{yy}^*/σ_y) so that Equation (7) will usually predict a decrease in toughness following an increase in strength.

The two microstructures, I and N, differ notably in the spacing of the grain boundary carbides that initiate cleavage; the spacing is $80 \mu\text{m}$ in microstructure I and $40 \mu\text{m}$ in N. If δ^* is scaled with this carbide

spacing, then, ignoring the differences in σ_y and σ_{yy}^* for the moment, we expect a $\sqrt{2}$ fold (i.e. ~41 percent) increase in toughness for microstructure I over that of microstructure N. According to Table III, the trend is indeed for an increase; however, except at -73°C , the observed increase is not as large as a factor of $\sqrt{2}$. The higher yield strength of microstructure I may account for this, since as noted above, a larger σ_y typically is associated with larger I^* and hence with a reduced toughness.

In summary then, the present results suggest that the simple fracture criterion proposed by Ritchie et al. for cleavage provides valuable insight into the effect of microstructure on the fracture toughness of pearlitic 1020 steel. We have found that it is possible starting with a normalized steel to obtain both higher toughness and higher strength by isothermally transforming to a ferritic-pearlitic microstructure. The increases in toughness are confined essentially to the temperature range -130°C to 18°C where fracture is by cleavage. At higher temperatures the toughnesses of the two microstructures is comparable, whereas the high rate strength is still higher for the isothermally formed microstructure. The increases in toughness are tentatively attributed to the increased spacing of grain boundary carbides.

Acknowledgement

The authors gratefully acknowledge the support of this research by the Army Research Office, grant DAAG29-80-K-0045, and the Materials Research Laboratory at Brown University funded by the National Science Foundation.

References

1. McMahon, C. J. Jr. and Cohen, M., "Initiation of Cleavage in Polycrystalline Iron," *Acta Metallurgica*, Vol. 13, 1965, pp. 591-604.
2. McMahon, C. J. Jr. and Cohen, M., "The Fracture of Polycrystalline Iron," *Proceedings of the First International Conference on Fracture*, Vol. 2, Sendai, Japan, pp. 779-812.
3. Costin, L. S. and Duffy, J., "The Effect of Loading Rate and Temperature on the Initiation of Fracture in a Mild Rate Sensitive Steel," *Transactions of the American Society of Mechanical Engineers, Journal of Engineering Material and Technology*, Vol. 101, 1979, pp. 258-264.
4. Wilson, M. L., Hawley, R. H. and Duffy, J., "The Effect of Loading Rate and Temperature on Fracture Initiation in 1020 Hot-Rolled Steel," *Engineering Fracture Mechanics*, Vol. 13, 1980, pp. 371-385.
5. Ritchie, R. O., Knott, J. F. and Rice, J. R., "On the Relationship Between Critical Tensile Stress and Fracture Toughness in Mild Steel," *Journal of the Mechanics and Physics of Solids*, Vol. 21, 1973, pp. 395-410.
6. Costin, L. S., Duffy, J. and Freund, L. B., "Fracture Initiation in Metals Under Stress Wave Loading Conditions," Fast Fracture and Crack Arrest, ASTM STP 627, G. T. Hahn and M. F. Kanninen, Eds., American Society for Testing and Materials, 1977, pp. 301-318.
7. Senseny, P. E., Duffy, J. and Hawley, R. H., "Experiments on Strain Rate History and Temperature Effects During the Plastic Deformation of Close Packed Metals," *Transactions of the American Society of Mechanical Engineers, Journal of Applied Mechanics*, Vol. 45, 1978; pp. 60-72.
8. Duffy, J., Campbell, J. D. and Hawley, R. H., "On the Use of a Torsional Split Hopkinson Bar to Study Rate Effects in 1100-0 Aluminum," *Transactions of the American Society of Mechanical Engineers, Journal of Applied Mechanics*, Vol. 38, 1971, pp. 83-91.
9. Tada, H., The Stress Analysis of Cracks Handbook, Del Research Corp., Hellertown, PA, 1973.
10. Rice, J. R., Paris, P. C. and Merkle, J. G., "Some Further Results in J-Integral Analysis and Estimates," Progress in Flaw Growth and Fracture Toughness Testing, ASTM STP 536, American Society for Testing and Materials; 1973, pp. 231-245.
11. McMeeking, R. M., "Finite Deformation Analysis of Crack Tip Opening in Elastic-Plastic Materials and Implications for Fracture Initiation," *Journal of the Mechanics and Physics of Solids*, Vol. 25, 1977, pp. 357-381.

Table I

<u>Composition of Steel</u>	
Carbon	0.22%
Manganese	0.47%
Phosphorus	0.01%
Sulphur	0.03%

Table II: Average microstructural characteristics of specimens employed in fracture tests.

Heat-treatment	N Normalized	I Isothermally Transformed
% Ferrite	73	72
% Pearlite	27	28
Mean radius of pearlite colonies	5.8 μm	5.2 μm
Mean spacing of pearlite colonies	24 μm	23 μm
Average thickness of carbide plates	1 μm	< 0.5 μm
Mean spacing of carbide plates	40 μm	80 μm

Table III: Stress intensity factor K_{Jc} for microstructures N and I

Temp.	$\sigma_y = \sqrt{3} \tau_y$ (MPa)		K_{Jc} (MPa \sqrt{m} s $^{-1/2}$)		percent increase in K_{Jc} due to isothermal trans.
	N	I	N	I	
-128C	793	862	26	32	23
-73C	634	703	26	39	50
-18C	565	600	43	57	33
+18C	469	538	58	58	-

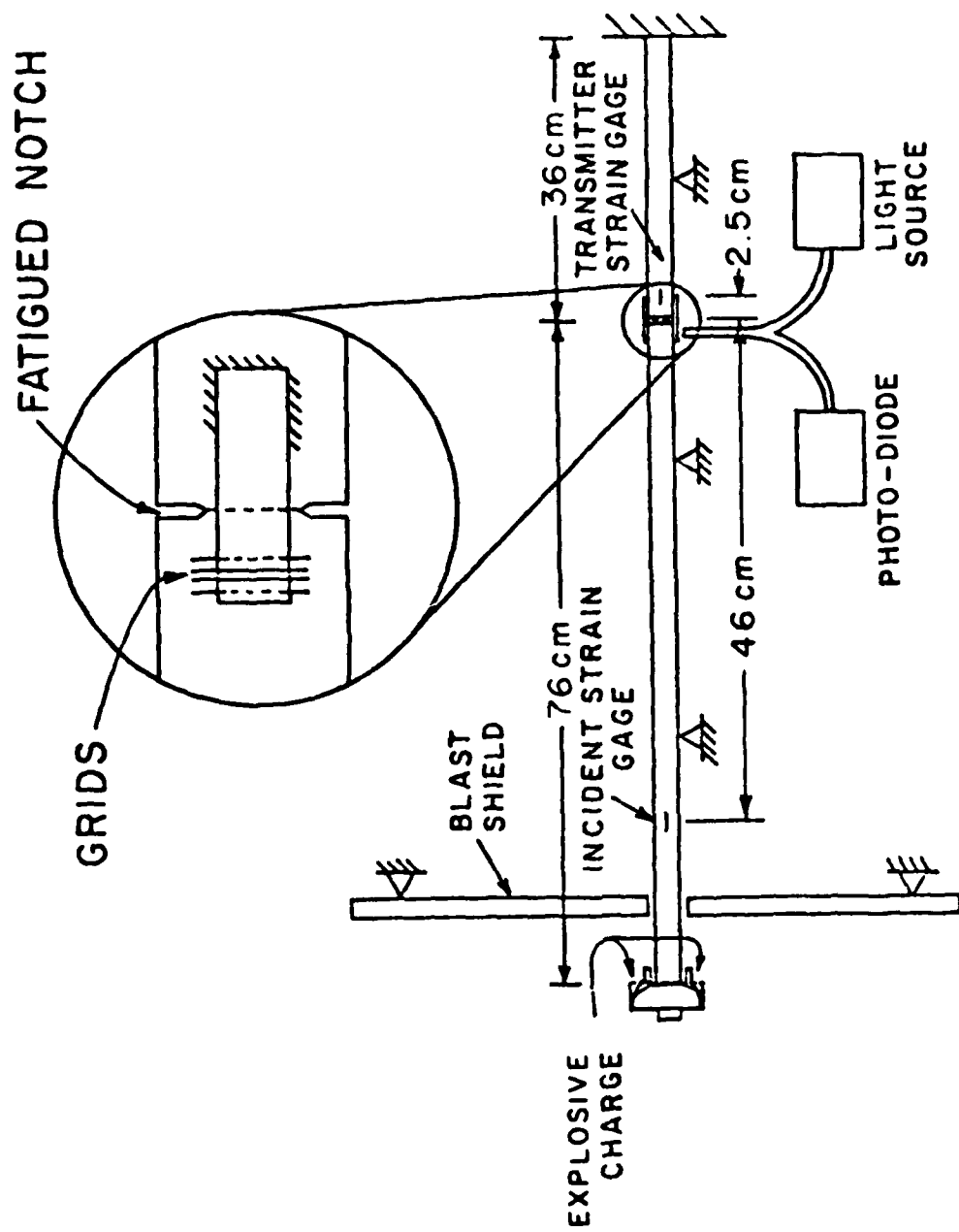


FIG.1 A SCHEMATIC DIAGRAM OF THE DYNAMIC FRACTURE APPARATUS ADAPTED FROM [3]

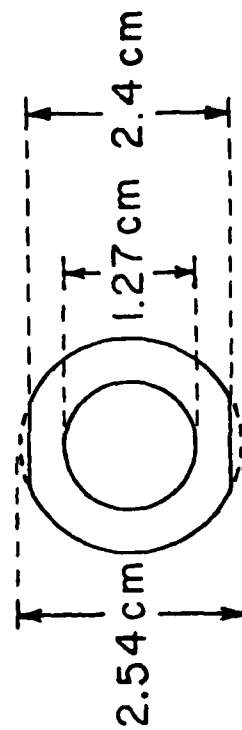
MACHINED FLATS
REQUIRED TO
ACCOMMODATE OPTICAL
DEVICE

60° INCLUDED ANGLE

2.54 mm

7 cm

7 cm



SECTION THROUGH NOTCH

FIG. 2 DETAILS OF THE NOTCHED REGION OF THE SPECIMEN. [4]

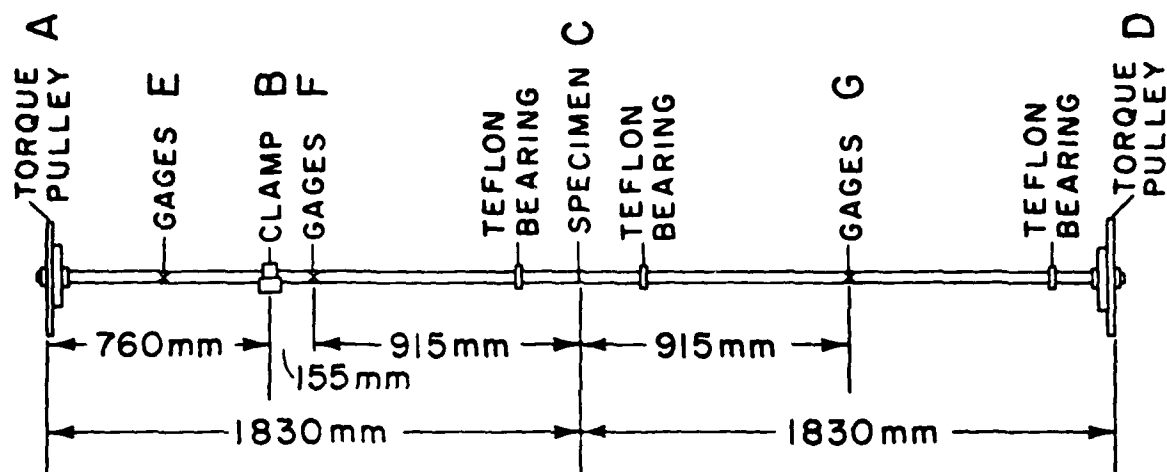


FIG. 3 SCHEMATIC DIAGRAM OF STORED TORQUE KOLSKY BAR (ADAPTED FROM [3])

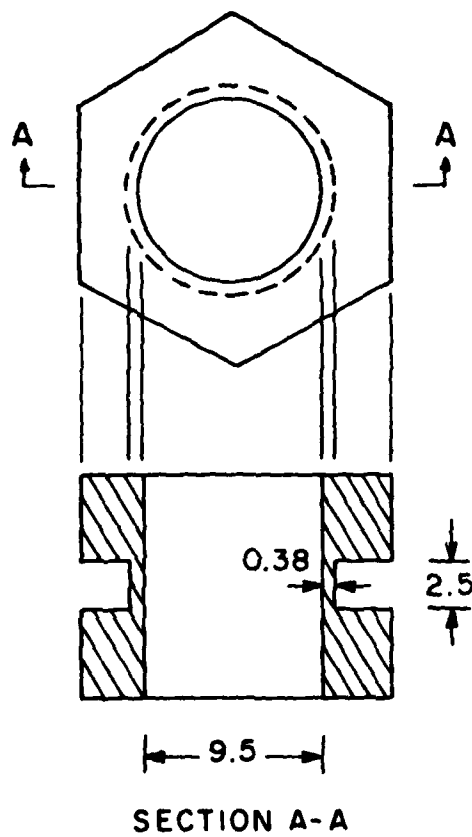
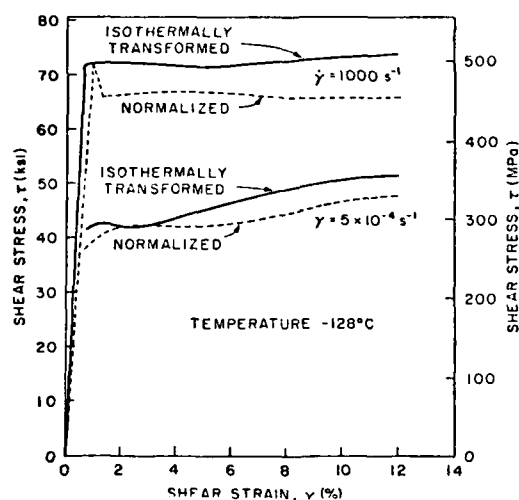
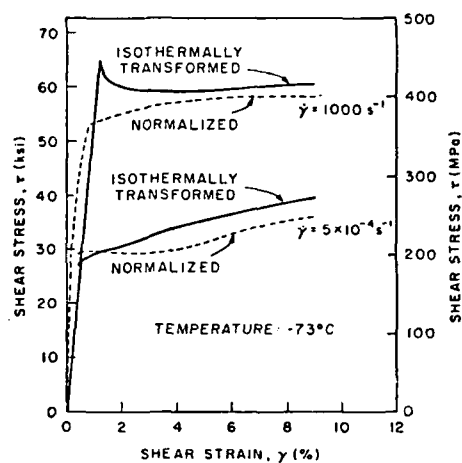


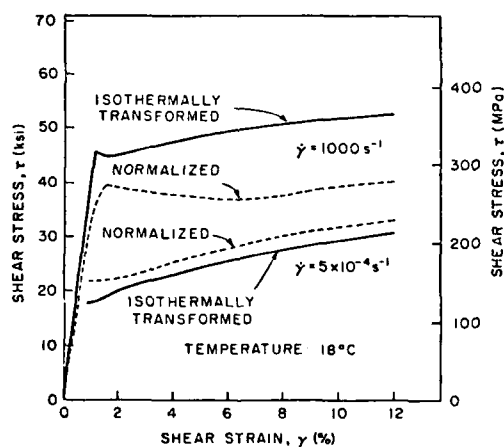
FIG. 4 DETAILS OF TORSIONAL SPECIMEN WITH HEXAGONAL MOUNTING FLANGES. DIMENSIONS ARE IN MILLI-METERS.



(a)



(b)

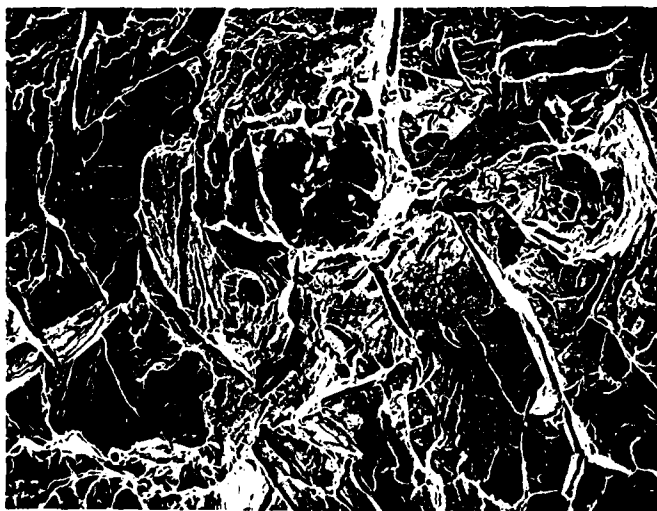


(c)

FIG. 5 DYNAMIC AND STATIC STRESS-STRAIN CURVES FOR NORMALIZED AND ISOTHERMALLY TRANSFORMED 1020 STEEL AT VARIOUS TEMPERATURES.



(a)
FRACTURE AT -101°C
x500



(b)
FRACTURE AT -18°C
x250

FIG. 6 SEM FRACTOGRAPHS SHOWING TRANSGRANULAR
CLEAVAGE IN ISOTHERMALLY TRANSFORMED
1020 HRS.

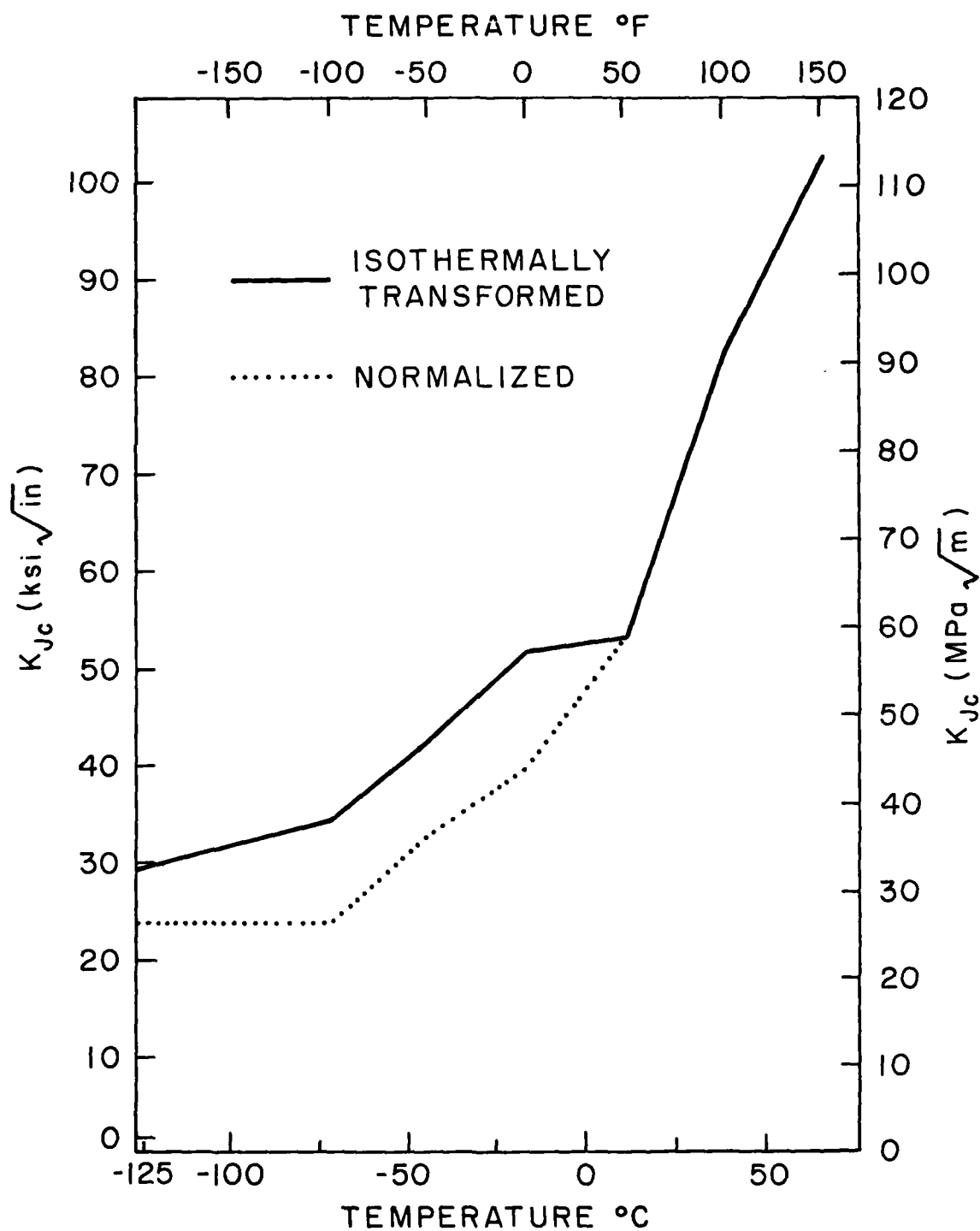


FIG. 7 FRACTURE TOUGHNESS OF NORMALIZED AND ISOTHERMALLY TRANSFORMED 1020 HRS VERSUS TEMPERATURE.

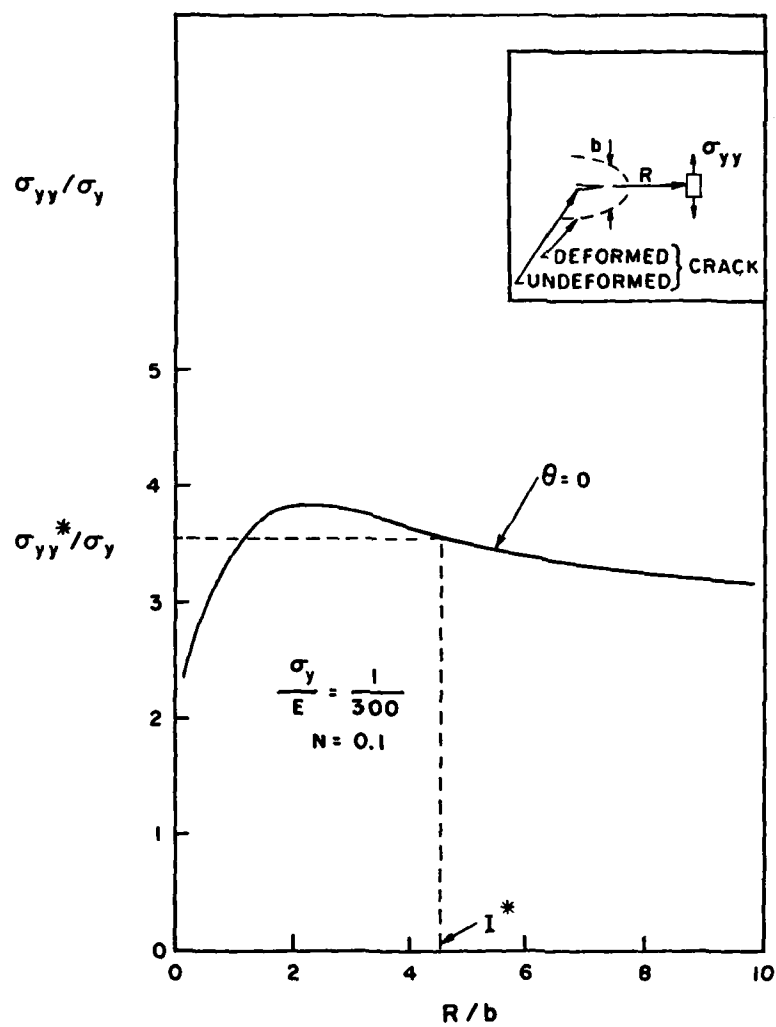


FIG. 8 PLOT OF CALCULATED STRESS σ_{yy}/σ_y NEAR THE BLUNTED CRACK TIP. (ADAPTED FROM [11]) N IS WORK HARDENING COEFFICIENT.

